Inorg. Chem. **2006**, *45*, 7511–7521

Forum

Solution–Liquid–Solid Growth of Semiconductor Nanowires

Fudong Wang, Angang Dong, Jianwei Sun, Rui Tang, Heng Yu, and William E. Buhro*

Department of Chemistry and Center for Materials Innovation, Washington University, St. Louis, Missouri 63130-4899

Received March 24, 2006

The serendipitously discovered solution–liquid–solid (SLS) mechanism has been refined into a nearly general synthetic method for semiconductor nanowires. Purposeful control of diameters and diameter distributions is achieved. The synthesis proceeds by a solution-based catalyzed-growth mechanism in which nanometer-scale metallic droplets catalyze the decomposition of metallo-organic precursors and crystalline nanowire growth. Related growth methods proceeding by the analogous vapor–liquid–solid (VLS) and supercritical fluid–liquid–solid (SFLS) mechanisms are known, and the relative attributes of the methods are compared. In short, the VLS method is most general and appears to afford nanowires of the best crystalline quality. The SLS method appears to be advantageous for producing the smallest nanowire diameters and for variation and control of surface ligation. The SFLS method may represent an ideal compromise. Recent results for SLS growth are summarized.

Introduction

This paper describes the development of an accidental discovery into a nearly general strategy for the synthesis of soluble (dispersible) semiconductor nanowires, having controlled diameters and narrow diameter distributions. The nanowires are grown by a catalyzed mechanism outlined below, named the "solution−liquid−solid" (SLS) mechanism[1] by analogy to the related, previously discovered vapor−liquid−solid (VLS) mechanism.[2] Other synthetic strategies for nanowires exist, such as template approaches, nanoparticle self-assembly (oriented attachment), vapor−solid growth, etc., as has been detailed elsewhere.[3,4] However, the variants of VLS growth in current use can provide advantages in nanowire crystallinity, length, and diameter control. The variants of VLS growth that are conducted in *solution*—SLS and supercritical fluid−liquid−solid (SFLS)[5] growth—additionally provide nanowire solubility, control over surface ligation, and small diameters in the range of ca. 4−12 nm, which are on the order of the exciton Bohr radii in common semiconductors. Because small-diameter nanowires passivated by traditional quantum-dot surfactants can now be grown by the SLS mechanism under conditions that closely approximate those for the growth of the best-quality quantum dots, the physical and spectroscopic properties of corresponding sets of quantum dots and quantum wires may now be directly compared.[6]

At the time of our initial discovery of SLS growth in the mid-1990s, we could not have imagined the interest that would arise in nanowires. Carbon nanotubes were first described by Iijima in 1991,[7] and the first reports of the VLS growth of semiconductor nanowires (having diameters of ≤20 nm) began to appear at about the same time.[8,9] Those discoveries seem to have nucleated a new research field. As shown in Figure 1, publications on nanowires or nanowhiskers rose from 1 in 1990 to nearly 3000 in 2005. This intense publication activity reflects the attention generated by the fundamental phenomena that nanowires exhibit, including

* To whom correspondence should be addressed. E-mail: buhro@wustl.edu.

(1) Trentler, T. J.; Hichman, K. M.; Goel, S. C.; Viano, A. M.; Gibbons, P. C.; Buhro, W. E. *Science* **1995**, *270*, 1791−1794.
(2) Wagner, R. S.; Ellis, W. C. *Appl. Phys. Lett.* **1964**, *4*, 89−90.
(3) Xia, Y.; Yang, P.; Sun, Y.; Wu, Y.; Mayers, B.; Gates, B.; Yin, Y.; Kim, F.; Yan, H. *Adv. Mater.* **2003**, *15*, 353−389.
(4) Law, M.; Goldberger, J.; Yang, P. *Annu. Rev. Mater. Res.* **2004**, *34*, 83−122.
(5) Hanrath, T.; Korgel, B. A. *Adv. Mater.* **2003**, *15*, 437−440.
(6) Yu, H.; Li, J.; Loomis, R. A.; Gibbons, O. C.; Wang, L.-W.; Buhro, W. E. *J. Am. Chem. Soc.* **2003**, *125*, 16168−16169.
(7) Iijima, S. *Nature* **1991**, *354*, 56−58.
(8) Yazawa, M.; Koguchi, M.; Hiruma, K. *Appl. Phys. Lett.* **1991**, *58*, 1080−1082.
(9) Yazawa, M.; Koguchi, M.; Muto, A.; Ozawa, M.; Hiruma, K. *Appl. Phys. Lett.* **1992**, *61*, 2051−2053.

10.1021/ic060498r CCC: $33.50
Published on Web 09/11/2006

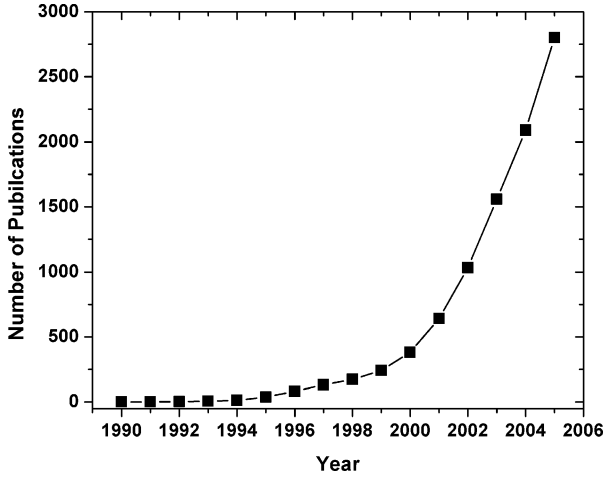

Figure 1. Number of publications on nanowires or nanowhiskers by year, determined from a CAS SciFinder search.

two-dimensional (2D) quantum confinement,[6,10,11] polarized luminescence,[12] lasing,[13,14] electrical transport,[15,16] and photoconductivity,[17] and the potential for nanowire applications in light emission,[18,19] chemical sensing,[20,21] nanophotonics,[22] photovoltaics,[17] and nanoelectronics.[15,16,18,23]

The focus here is on the synthetic aspects of SLS growth and related methods. We begin with a historical overview of our elucidation and development of the SLS mechanism. Contributions to this general area have been made by Ahrenkiel,[24] Banin,[25,26] Korgel,[5,27−32] Kuno,[33,34] Lieber,[35−39] Mićić,[40] Xie,[41−43] Yang,[44−46] and others, which are noted. We then provide a summary of our new synthetic results.

Historical Overview

Discovery of the SLS Mechanism. In the early 1990s, we were interested in the synthesis of phosphide and arsenide nanocrystals (sometimes referred to as quantum dots; we will use these terms interchangeably). Great progress had been made at that time in the synthesis of high-quality II−VI (12−16) nanocrystals, such as CdSe quantum dots.[47,48] However, syntheses of II_3-V_2 (12_3-15_2) and III−V (13−15) nanoparticles such as those composed of Cd_3P_2, InP, and GaAs were considerably less advanced.[47−51] Interestingly, to our knowledge, high-quality (crystalline, soluble, narrowly dispersed, and highly emissive) quantum dots of Cd_3P_2 and GaAs have not yet been prepared, more than a decade later.

Our strategy involved elaborate, synthetically intensive, single-source precursors, like compounds **1** and **2**, designed to undergo condensation−elimination reactions in solution to afford semiconductor nanocrystals.[52−55] Closely related

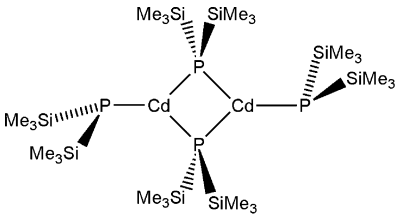

1 **2**

studies were undertaken by Theopold and Douglas.[56−58] Our early efforts sometimes gave semiconductor nanoparticles,

(10) Yu, H.; Li, J.; Loomis, R. A.; Wang, L.-W.; Buhro, W. E. *Nat. Mater.* **2003**, *2*, 517−520.
(11) Gudiksen, M. S.; Wang, J.; Lieber, C. M. *J. Phys. Chem. B* **2002**, *106*, 4036−4039.
(12) Wang, J.; Gudikson, M. S.; Duan, X.; Cui, Y.; Lieber, C. M. *Science* **2001**, *293*, 1455−1457.
(13) Huang, M.; Mao, S.; Feick, H.; Yan, H.; Wu, Y.; Kind, H.; Weber, E.; Russo, R.; Yang, P. *Science* **2001**, *292*, 1897−1899.
(14) Duan, X.; Huang, Y.; Agarwal, R.; Lieber, C. M. *Nature* **2003**, *421*, 241−245.
(15) Cui, Y.; Lieber, C. M. *Science* **2001**, *291*, 851−853.
(16) Cui, Y.; Duan, X.; Hu, J.; Lieber, C. M. *J. Phys. Chem. B* **2000**, *104*, 5213−5216.
(17) Law, M.; Greene, L.; Johnson, J. C.; Saykally, R.; Yang, P. *Nat. Mater.* **2005**, *4*, 455−459.
(18) Duan, X.; Huang, Y.; Cui, Y.; Wang, J.; Lieber, C. M. *Nature* **2001**, *409*, 66−69.
(19) Gudikson, M. S.; Lauhon, L. J.; Wang, J.; Smith, D. C.; Lieber, C. M. *Nature* **2002**, *415*, 617−620.
(20) Cui, Y.; Wei, Q. Q.; Park, H. K.; Lieber, C. M. *Science* **2001**, *293*, 1289−1292.
(21) Law, M.; Kind, H.; Messer, B.; Kim, F.; Yang, P. *Angew. Chem., Int. Ed.* **2002**, *41*, 2405−2408.
(22) Law, M.; Sirbuly, D. J.; Johnson, J. C.; Goldberger, J.; Saykally, R. J.; Yang, P. *Science* **2004**, *305*, 1269−1273.
(23) Huang, Y.; Duan, X.; Cui, Y.; Lauhon, L. J.; Kim, K.-H.; Lieber, C. M. *Science* **2001**, *294*, 1313−1317.
(24) Ahrenkiel, S. P.; Mićić, O. I.; Miedaner, A.; Curtis, C. J.; Nedeljković, J. M.; Nozik, A. J. *Nano Lett.* **2003**, *3*, 833−837.
(25) Kan, S.; Mokari, T.; Rothenberg, E.; Banin, U. *Nat. Mater.* **2003**, *2*, 155−158.
(26) Kan, S.; Aharoni, A.; Mokari, T.; Banin, U. *Faraday Discuss.* **2004**, *125*, 23−38.
(27) Lu, X.; Fanfair, D. D.; Johnston, K. P.; Korgel, B. A. *J. Am. Chem. Soc.* **2005**, *127*, 15718−15719.
(28) Fanfair, D. D.; Korgel, B. A. *Cryst. Growth Des.* **2005**, *5*, 1971−1976.
(29) Holmes, J. D.; Johnston, K. P.; Doty, R. C.; Korgel, B. A. *Science* **2000**, *287*, 1471−1473.
(30) Hanrath, T.; Korgel, B. A. *J. Am. Chem. Soc.* **2002**, *124*, 1424−1429.
(31) Dadidson, F. M., III; Schricker, A. D.; Wiacek, R. J.; Korgel, B. A. *Adv. Mater.* **2004**, *16*, 646−649.
(32) Dadidson, F. M., III; Wiacek, R. J.; Korgel, B. A. *Chem. Mater.* **2005**, *17*, 230−233.
(33) Grebinski, J. M.; Hull, K. L.; Zhang, J.; Kosel, T. H.; Kuno, M. *Chem. Mater.* **2004**, *16*, 5260−5272.
(34) Hull, K. L.; Grebinski, J. M.; Zhang, J.; Kosel, T. H.; Kuno, M. *Chem. Mater.* **2005**, *17*, 4416−4425.
(35) Morales, A. M.; Lieber, C. M. *Science* **1998**, *279*, 208−211.
(36) Gudiksen, M. S.; Lieber, C. M. *J. Am. Chem. Soc.* **2000**, *122*, 8801−8802.
(37) Duan, X.; Lieber, C. M. *Adv. Mater.* **2000**, *12*, 298−302.
(38) Cui, Y.; Lauhon, L. J.; Gudiksen, M. S.; Wang, J.; Lieber, C. M. *Appl. Phys. Lett.* **2001**, *78*, 2214−2216.
(39) Gudiksen, M. S.; Wang, J.; Lieber, C. M. *J. Phys. Chem. B* **2001**, *105*, 4062−4064.
(40) Nedeljković, J. M.; Mićić, O. I.; Ahrenkiel, S. P.; Miedaner, A.; Nozik, A. J. *J. Am. Chem. Soc.* **2004**, *126*, 2632−2639.
(41) Lu, J.; Xie, Y.; Jiang, X.; He, W.; Yan, P.; Qian, Y. *Can. J. Chem.* **2001**, *79*, 127−130.
(42) Xiao, J.; Xie, Y.; Tang, R.; Qian, Y. *J. Solid State Chem.* **2001**, *161*, 179−183.
(43) Gao, S.; Xie, Y.; Lu, J.; Du, G.; He, W.; Cui, D.; Huang, B.; Jiang, M. *Inorg. Chem.* **2004**, *41*, 1850−1854.
(44) Wu, Y.; Yang, P. *J. Am. Chem. Soc.* **2001**, *123*, 3165−3166.
(45) Yang, P.; Yan, H.; Mao, S.; Russo, R.; Johnson, J.; Saykally, R.; Morris, N.; Pham, J.; He, R.; Choi, H.-J. *Adv. Funct. Mater.* **2002**, *12*, 323−331.
(46) Wu, Y.; Yan, H.; Huang, M.; Messer, B.; Song, J. H.; Yang, P. *Chem.−Eur. J.* **2002**, *8*, 1260−1268.
(47) Murray, C. B.; Norris, D. J.; Bawendi, M. G. *J. Am. Chem. Soc.* **1993**, *115*, 8706−8715.
(48) Bowen Katari, J. E.; Colvin, V. L.; Alivisatos, A. P. *J. Phys. Chem.* **1994**, *98*, 4109−4117.
(49) Olshavsky, M. A.; Goldstein, A. N.; Alivisatos, A. P. *J. Am. Chem. Soc.* **1990**, *112*, 9438−9439.
(50) Uchida, H.; Curtis, C. J.; Nozik, A. J. *J. Phys. Chem.* **1991**, *95*, 5382−5384.

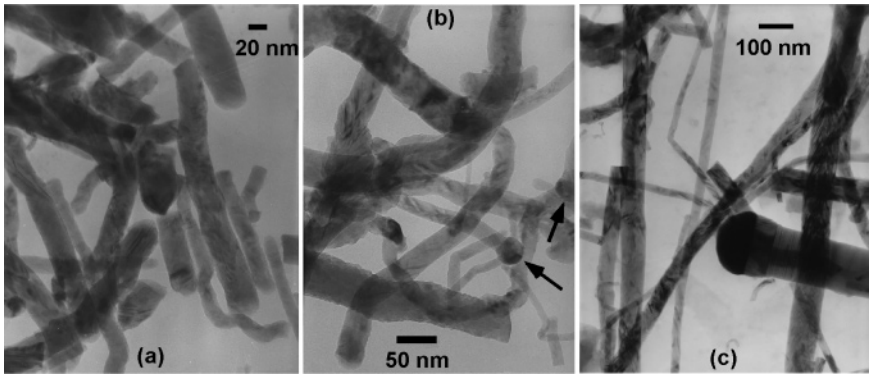

Figure 2. TEM images of crystalline InP fibers: (a) from methanolysis of **2** (R = *t*-Bu); (b) under conditions allowing the imaging of the In-catalyst droplets (arrows); (c) from a higher-temperature synthesis employing added In catalyst.

but they were insoluble, amorphous (noncrystalline), and exhibited a wide distribution of sizes.[53,55] Furthermore, mechanistic studies, by us[54] and by Theopold and Douglas,[57,58] indicated that the reactions proceeded through intermediates that could also be generated from much simpler precursors. We had misdiagnosed the problem. Precursor decomposition to a semiconductor of the desired stoichiometry was a necessary but insufficient condition; an active crystal-growth mechanism was *also* necessary but absent under the reaction conditions employed. With a crystal-growth mechanism in place, we could next tackle the issues of solubility and size control. However, we had no good ideas for activating crystal growth, except to raise the reaction temperature, which was unsuccessful in our hands.

Even a blind pig occasionally finds an acorn. We had the good fortune to investigate the methanolysis reaction of a specific derivative of precursor **2** (R = *t*-Bu), in refluxing toluene.[54,55] An X-ray diffraction pattern of the black, insoluble product indicated that *crystalline* InP had formed, along with a small amount of metallic In from a side reaction. A transmission electron microscopy (TEM) image of the black solid contained irregular, kinky, polycrystalline *fibers* of varying diameter and length (Figure 2a). Although a crystal-growth mechanism had obviously been activated, resulting in the polycrystalline InP fibers, its origin and characteristics were a mystery.

A literature search led us to mechanisms for whisker growth, of which only two were commonly cited, the screw-dislocation mechanism[59,60] and the VLS mechanism. The VLS mechanism is thought to be responsible for most observations of whisker growth from the vapor[60] and was proposed by Wagner and Ellis[2] in 1964 to account for the growth of Si whiskers on Au-decorated Si substrates under chemical vapor deposition (CVD) conditions. In their proposal, Au particles deposited on Si melt to variously sized Au droplets at the elevated temperature of a CVD reactor. Admission of a gaseous mixture of $SiCl_4$ and H_2 results in preferential reaction at the Au−droplet interface, with the dissolution of elemental Si into the Au droplet. When a droplet achieves Si supersaturation, a crystalline Si whisker is nucleated at the droplet−substrate interface (Figure 3a). Because the resulting droplet−whisker interface is the most active crystal-growth interface, the growing whisker naturally acquires a pseudo-one-dimensional (1D) morphology and continues growing until the precursor delivery is discontinued. The Au droplet catalyzes whisker growth in part by functioning as a crystallization solvent. Wagner and Ellis named the VLS mechanism after the three phases involved: the *vapor*-phase precursor, the *liquid* catalyst droplet, and the *solid* crystalline product. The VLS mechanism was subsequently recognized to promote whisker growth for a wide range of elements and compounds, generally giving mean whisker diameters of ≥100 nm and wide diameter distributions.[59,60]

We considered the possibility that a VLS-like mechanism might be responsible for InP fiber formation under our lower-temperature, solution-phase conditions.[54] As noted above, metallic In (mp = 157 °C) was a persistent side product and could potentially provide the necessary liquid catalyst droplets. However, metallic In was not initially evident in TEM images obtained under normal circumstances (Figure 2a), because it rapidly melted under e-beam irradiation and scattered from the field of view. Consequently, we re-imaged InP samples at lower e-beam current densities in a liquid-N_2-cooled TEM sample holder. Such images revealed frozen In droplets fused to the ends of InP fibers (see Figure 2b). Furthermore, we observed that InP precursors that failed to give metallic In as a side product also failed to give polycrystalline InP fibers. However, such reactions could often be activated for InP growth by the *addition* of metallic

(51) Mićić, O. I.; Curtis, C. J.; Jones, K. M.; Sprague, J. R.; Nozik, A. J. *J. Phys. Chem.* **1994**, *98*, 4966−4969.
(52) Goel, S. C.; Chiang, M. Y.; Buhro, W. E. *J. Am. Chem. Soc.* **1990**, *112*, 5636−5637.
(53) Matchett, M. A.; Viano, A. M.; Adolphi, N. L.; Stoddard, R. D.; Buhro, W. E.; Conradi, M. S.; Gibbons, P. C. *Chem. Mater.* **1992**, *4*, 508−511.
(54) Trentler, T. J.; Goel, S. C.; Hickman, K. M.; Viano, A. M.; Chiang, M. Y.; Beatty, A. M.; Gibbons, P. C.; Buhro, W. E. *J. Am. Chem. Soc.* **1997**, *119*, 2172−2181.
(55) Buhro, W. E. *Polyhedron* **1994**, *13*, 1131−1148.
(56) Byrne, E. K.; Parkanyi, L.; Theopold, K. H. *Science* **1988,** *241*, 332−334.
(57) Douglas, T.; Theopold, K. H. *Inorg. Chem.* **1991**, *30*, 594−596.
(58) Douglas, T. Ph.D. Thesis, Cornell University, Ithaca, NY, 1991.
(59) Wagner, R. S. In *Whisker Technology*; Levitt, A. P., Ed.; Wiley: New York, 1970; Chapter 3.
(60) Givargizov, E. I. In *Current Topics in Materials Science*; Kaldis, E., Ed.; North-Holland: Amsterdam, The Netherlands, 1978; Vol. 1, Chapter 3.

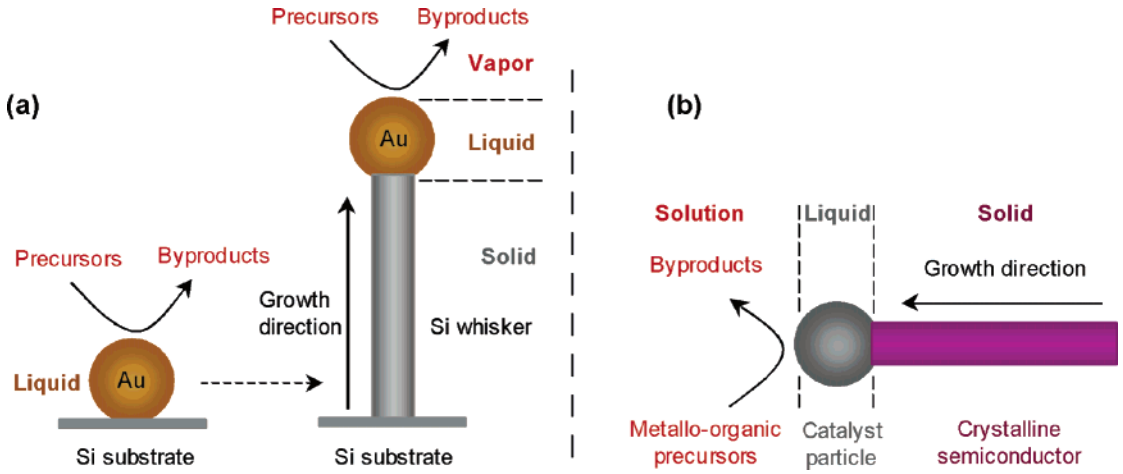

Figure 3. Growth mechanisms for pseudo-1D crystalline morphologies: (a) VLS mechanism proposed by Wagner and Ellis for growth under CVD conditions; (b) SLS mechanism proposed by Buhro and co-workers for analogous growth from solution.

In. Longer, straighter nanowires were obtained at higher growth temperatures of ~200 °C (Figure 2c), the best of which approached single-crystal character, apart from stacking faults.[1] The In alloy catalyst particles found on the nanowires grown at higher temperatures were more thermally robust and could be imaged under normal conditions. We were also able to grow crystalline GaAs,[1] InAs,[1] and $Al_xGa_{1-x}As$[61] nanowires similarly and found catalyst particles attached to the wire tips. All of the experimental results taken together provided strong support for a VLS-like mechanism, which we named the SLS mechanism to distinguish between precursor delivery from solution and the vapor phase (Figure 3b).[1,54]

There exist strong indications that the catalyst droplets in the VLS and SLS mechanisms play a catalytic role in precursor decomposition, in addition to catalyzing wire growth. The early VLS literature claimed such a role on the basis of various experimental observations,[2,59,60] including that VLS crystal growth typically occurs at temperatures several hundreds of degrees lower than epitaxial film growth from the same precursors.[59] Indeed, if precursor decomposition were uncatalyzed, then deposition would occur indiscriminately, and film growth would compete with VLS wire growth. Our study of the SLS growth of InP fibers established that metallic In catalyzed precursor decomposition, which was incomplete in the *absence* of In under the same conditions.[54] As above, if precursor decomposition were uncatalyzed, then the formation of an amorphous or nanocrystalline semiconductor would compete with SLS wire growth. In one case (discussed later), we found that the homogeneous nucleation of InP rod clusters competed with SLS wire growth. However, that competing process was quenched by the addition of an inhibitor to the growth of the homogeneous nuclei, allowing precursor decomposition to occur more rapidly upon the SLS catalyst droplets. Thus, the droplets perform a dual role as ideally rough surfaces[59,60] for precursor adsorption and decomposition and as a crystallization solvent supporting semiconductor crystal-lattice formation and, hence, wire growth.

Our observations of SLS growth, reported in 1995,[1] were likely not the first. In 1993, Heath and LeGoues described a solution synthesis of single-crystal Ge quantum wires by Na reduction of $GeCl_4/PhGeCl_3$ mixtures in a sealed pressure bomb at 275 °C.[62] The wires exhibited diameters of 7−30 nm and were micrometers in length. Na catalyst particles were not observed at the ends of the wires but would have been removed by the workup procedures employed. No analogy to VLS growth was suggested, but the authors reported that the wires did not contain screw dislocations. We surmise that they likely grew by the SLS mechanism. Other prior examples of SLS growth may exist that we are unaware of.

Having found a mechanism for growing 1D semiconductor "wires", our interests turned to investigating quantum-confinement effects in wires rather than dots. However, as is evident in Figure 2, the nanowire mean diameters were far too large and the diameter distributions far too broad for studies of quantum confinement in ensembles of wires. Controlled diameters in the range of ca. 2−12 nm and narrow diameter distributions were required for such studies. Additionally, the crystalline quality of the wires was insufficient, and they were insoluble, precluding solution spectroscopy. We reasoned that the diameters of the wires should depend on the diameters of the catalyst particles from which they grew and therefore that near-monodisperse catalyst particles over a range of appropriate sizes would be necessary for SLS growth of high-quality quantum-wire specimens.

Melting points, solvating abilities, and reactivities are the important criteria for judging candidate metals or metal alloys as potential VLS or SLS catalyst materials. Catalyst particles must be molten under the reaction conditions. Because we wished to use reaction temperatures in the range of ca. 200−300 °C, metal nanoparticles melting in that range would be required. Additionally, at least one of the components of the product semiconductor phase must have finite but limited

(61) Markowitz, P. D.; Zach, M. P.; Gibbons, P. C.; Penner, R. M.; Buhro, W. E. *J. Am. Chem. Soc.* **2001**, *123*, 4502−4511.

(62) Heath, J. R.; LeGoues, F. K. *Chem. Phys. Lett.* **1993**, *208*, 263−268.

solubility in the catalyst material, so that high supersaturations can be achieved. For the III−V and II−VI semiconductors discussed here, the group V or VI element has the limiting solubility. Finally, the catalyst should not react with or form a solid solution with the target semiconductor phase (unless the catalyst material is the *same* as one of the constituent elements of the semiconductor). The low-melting metals best meeting these three criteria seemed to be In, Bi, and Sn. Therefore, we sought near-monodisperse In, Bi, and Sn nanoparticles having controlled diameters in the range of ca. 5−25 nm, for use as SLS catalysts. Unfortunately, such nanoparticles were then unavailable. We decided to pursue them.

SFLS Growth of Semiconductor Nanowires. While our work on In, Bi, and Sn nanoparticle catalysts was in progress, Korgel and co-workers reported a breakthrough in controlled-diameter nanowire synthesis (in the year 2000).[29] Whereas monodisperse nanoparticles of low-melting metals were unavailable, monodisperse Au nanoparticles were readily available. The higher melting temperatures of Au nanoparticles required higher reaction temperatures, and thus supercritical-solvent conditions were employed. Si nanowires having diameters in the range of 4−5 nm, narrow diameter distributions (standard deviation $\leq \pm 10\%$ of the mean nanowire diameter), and aspect ratios of >1000 were grown from monodisperse 2.5-nm Au-catalyst particles in supercritical hexane at 500 °C and 200−270 bar. Significantly, the first spectroscopic evidence of quantum confinement in colloidal quantum wires was reported in this seminal study. The preparation of narrowly dispersed Si quantum wires over a range of diameters was not initially reported.

Korgel and co-workers subsequently extended the supercritical synthesis to Ge,[5,30] GaAs,[31] and GaP[32] nanowires. They named the method "supercritical fluid−liquid−solid" (SLFS)[5] growth to distinguish it from the VLS and SLS variations. In 2003, the group reported that the diameters of Si and Ge nanowires could be rationally controlled over the range of 4−30 nm by varying the size of the Au-catalyst nanoparticles employed.[5] As these advances were made, parallel developments were underway in the VLS and SLS syntheses of semiconductor nanowires, discussed below. A comparison of the relative attributes of the three strategies will ultimately follow.

VLS Growth of Semiconductor Nanowires. As noted above, the VLS method as originally practiced gave primarily large-diameter whiskers and wide diameter distributions. To our knowledge, the first indications of the VLS growth of semiconductor wires with nanometer-scale diameters were published in 1991 and 1992.[8,9] However, a very important study of VLS nanowire synthesis was published by Morales and Lieber in 1998,[35] which captured the interest and attention of the nanoscience research community. Nanowires of Si or Ge were prepared by laser ablation of Si or Ge targets containing 1−10% of a catalytic metal such as Fe, Ni, or Au. The metallic component condensed first from the target-derived vapor into nanoscale droplets, providing catalytic sites for the subsequent condensation and adsorption of Si or Ge. A carrier gas swept the ablated vapor through a 1200 °C furnace, where VLS growth of the nanowires occurred. The Si or Ge nanowires, collected from a coldfinger, had diameters in the range of 3−20 nm and lengths of 1−30 μm. Because there was no control over the size of the condensing metallic catalyst droplets, the diameter distributions in the products were broad. However, the crystalline quality of the nanowires was uniformly high. Duan and Lieber[37] extended this method, which they named the "laser-assisted catalytic-growth" (LCG) method, to the synthesis of several binary and ternary III−V, binary II−VI, and Si_xGe_{1-x} nanowires, demonstrating its generality.

Within a few months of the appearance of Korgel's original breakthrough in 2000, Gudiksen and Lieber reported an analogous solution to the diameter-control problem.[36] The LCG method was adapted for the use of presynthesized, monodisperse, Au-catalyst nanoparticles, which were deposited on a silica substrate and positioned within the furnace and carrier-gas flow. A GaP target was ablated and the vapor passed over the monodisperse catalyst, whereupon VLS growth of GaP nanowires ensued. The resulting diameter distributions were shown to be narrow ($\pm 5-17\%$ of the mean nanowire diameters) and to scale with the size of the catalyst nanoparticles. Significantly, Gudiksen and Lieber had therefore demonstrated for the first time the ability to control nanowire diameters, while maintaining narrow diameter distributions, over a *range* of diameters (in this case 11−30 nm). This method was subsequently extended to the control of the lengths and diameters of VLS-grown InP nanowires.[39]

In 2001, Wu and Yang reported diameter control in VLS-grown Si nanowires using monodisperse Au-catalyst nanoparticles of various sizes.[44] In the same study, they described the first real-time monitoring, by TEM imaging, of VLS Ge-nanowire growth. The growth process was found to consist of three distinct stages: catalyst−nanoparticle alloying, nanowire nucleation, and nanowire axial growth. Interestingly, the initial alloying stage was accompanied by a significant swelling of the catalyst nanoparticle as it dissolved Ge to the extent of 40−50 wt %, prior to reaching supersaturation and the nucleation stage. This accounts for the observation that the diameters of VLS-grown nanowires are generally *larger* than those of the catalyst nanoparticles from which they grew. Lieber and co-workers also reported diameter control in VLS-grown Si nanowires from monodisperse Au-catalyst nanoparticles, at about the same time as Wu and Yang's report.[38]

Yang and co-workers later reported VLS growth of other semiconductor nanowires. They achieved diameter control in the synthesis of ZnO nanowires, using the method described above.[45] They also monitored in real time the self-catalyzed VLS growth of GaN nanowires (from Ga droplets).[63] The Yang and Lieber groups separately described the VLS growth of compositionally modulated heterostructured nanowires, in which the composition was purposefully alternated along the axial dimension of the nanowire.[19,64]

(63) Stach, E. A.; Pauzauskie, P. J.; Kuykendall, T.; Goldberger, J.; He, R.; Yang, P. *Nano Lett.* **2003**, *3*, 867−869.
(64) Wu, Y.; Fan, R.; Yang, P. *Nano Lett.* **2002**, *2*, 83−86.

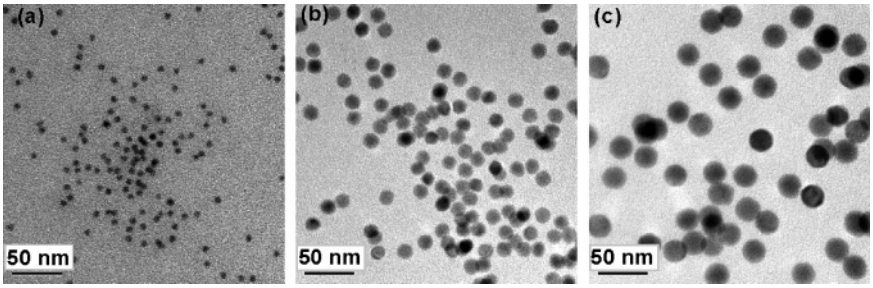

Figure 4. TEM images of near-monodisperse Bi nanoparticles obtained by thermal decomposition of $Bi[N(SiMe_3)_2]_3$ with $Na[N(SiMe_3)_2]$. The quantity following the ± symbol is 1 standard deviation in the diameter distribution, expressed as a percentage of the mean diameter. Mean diameter = (a) 6.4 nm ± 11.5%, (b) 15.1 nm ± 5.6%, and (c) 25.2 nm ± 5.1%.

They reported the construction of core−sheath (shell) heterostructures from VLS-grown nanowires, in which compositional discontinuities were incorporated into the radial dimension.[65−67] Most importantly, the Lieber and Yang groups have used such materials to study a wide range of fundamental nanowire phenomena,[11−17] to construct and demonstrate a variety of electronic,[15,18,23] electrooptic,[18,19] optical,[17,22] and nanofluidic[68] devices, and to investigate numerous potential nanowire applications.[15,17−23,68] One should certainly ascribe a large fraction of the interest in nanowire science evidenced in Figure 1 to the work of these two groups.

SLS Growth of Semiconductor Nanowires. As noted above, the SLS method initially gave semiconductor nanowires with insufficient diameter control and crystalline quality. Our strategy for diameter control was essentially the same as that above, except for the use of low-melting catalyst nanoparticles rather than the readily available Au nanoparticles. In 2001, we succeeded in the preparation of near-monodisperse In, Bi, and Sn nanoparticles using a seeded-growth method, in which very small ($d \approx 1.5$ nm) Au nanoclusters served as heterogeneous nucleants for nanoparticle growth.[69] Because we controlled the number of Au seeds employed, and therefore the number of growing nanoparticles, and because we also controlled the amounts of In, Bi, or Sn precursor added, we could predict with reasonable precision the ultimate sizes of the nanoparticles. Controlled diameters in the range of ca. 5−25 nm were achieved, with the standard deviations in the diameter distributions being 5−13% of the nanoparticle mean diameters (without fractional−crystallization distribution sharpening).

We have subsequently found that Bi nanoparticles seem to be the most generally useful for the diameter-controlled SLS growth of semiconductor nanowires. The heterogeneous seeded-growth synthesis of Bi nanoparticles was somewhat laborious and provided a limited size range. Consequently, we have developed a convenient one-pot synthesis of near-monodisperse Bi nanoparticles by *homogeneous* nucleation and growth using the thermal decomposition of $Bi[N(SiMe_3)_2]_3$ in the presence of $Na[N(SiMe_3)_2]$ (see Figure 4). This method affords nanoparticles in the diameter range of 4−40 nm, with standard deviations in the diameter distributions of 4−12% of the nanoparticle mean diameters. The Bi nanoparticles can be made on a large scale and stored for at least a few years under an inert atmosphere. We now use these Bi nanoparticles almost exclusively for the SLS growth of nanowires and expect that they may become generally useful to others. Thus, we intend to publish the synthesis soon, after a mechanistic study of the growth process is complete.

In 2003, we reported the diameter-controlled growth of crystalline InP quantum wires using near-monodisperse In-catalyst nanoparticles and the single-source precursor **2** (R = Me), at the comparatively low reaction temperature of 203 °C.[10] Large amounts of a polymer surfactant, poly(1-hexadecene-*co*-vinylpyrrolidinone), were employed to retain nanowire solubility. The nanowires had lengths of several micrometers and diameters that varied systematically in the range of 3.5−11 nm with the size ($d = 4.5$−21 nm) of the In-catalyst nanoparticles employed. Thus, the nanowire diameters were *smaller* than the diameters of the catalyst nanoparticles. Standard deviations in the diameter distributions were 13−21% of the mean nanowire diameter, which were reasonably narrow. The band gaps of the wires were measured spectroscopically and compared to those of InP quantum dots and theoretical predictions. Soluble GaAs nanowires were prepared similarly, with similar results.[70] These examples first demonstrated that SLS-nanowire growth can afford the systematic diameter control and narrow size distributions achievable by VLS and SLFS growth.

In 2003, we also reported SLS growth of soluble, diameter-controlled CdSe quantum wires from near-monodisperse Bi-catalyst nanoparticle.[6] The precursors and reaction conditions were adapted from Peng's synthesis of CdSe quantum dots.[71] Notably, polymer surfactants were not employed but rather the typical quantum-dot surfactants tri-*n*-octylphosphine oxide (TOPO), tri-*n*-octylphosphine (TOP), and *n*-hexadecylamine (HDA). The wires exhibited lengths of one to several micrometers and diameters in the range of 5−20 nm.

(65) Goldberger, J.; He, R.; Zhang, Y.; Lee, S.; Yan, H.; Choi, H.-J.; Yang, P. *Nature* **2003**, *422*, 599−602.
(66) Wu, Y.; Xiang, J.; Yang, C.; Lu, W.; Lieber, C. M. *Nature* **2004**, *430*, 61−65.
(67) Qian, F.; Li, Y.; Gradecak, S.; Wang, D.; Barrelet, C. J.; Lieber, C. M. *Nano Lett.* **2004**, *4*, 1975−1979.
(68) Karnik, R.; Fan, R.; Yue, M.; Li, D.; Yang, P.; Majumdar, A. *Nano Lett.* **2005**, *5*, 943−948.
(69) Yu, H.; Gibbons, P. C.; Kelton, K. F.; Buhro, W. E. *J. Am. Chem. Soc.* **2001**, *123*, 9198−9199.
(70) Yu, H.; Buhro, W. E. *Adv. Mater.* **2003**, *15*, 416−419.
(71) Peng, Z. A.; Peng, X. *J. Am. Chem. Soc.* **2001**, *123*, 183−184.

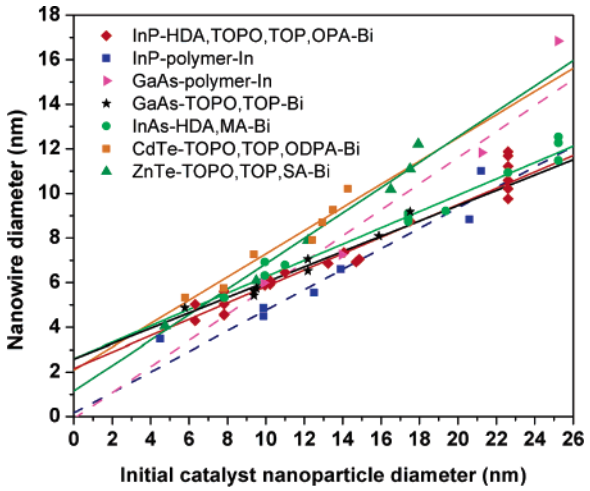

Figure 5. Plots of nanowire diameter vs initial catalyst nanoparticle diameter for SLS-grown wires. The lines are least-squares fits to the data, which are identified in the inset legend. The dotted lines correspond to nanowires grown from In-catalyst nanoparticles. Legend format: nanowire composition − surfactant list − catalyst-nanoparticle composition. HDA = *n*-hexadecylamine, TOPO = tri-*n*-octylphosphine oxide, TOP = tri-*n*-octylphosphine, OPA = *n*-octylphosphonic acid, MA = myristate, SA = stearate, and polymer = poly(1-hexadecene-*co*-vinylpyrrolidinone) for InP and poly(1-diphenylphosphinomethyl-4-vinylbenzene)/poly(1-hexadecene-*co*-vinylpyrrolidinone) mixtures for GaAs.

Standard deviations in the diameter distributions were 10−20% of the mean diameter. The wires achieved near-single-crystal character at the growth temperatures of 240−300 °C, although stacking faults were often evident. Band gaps were again measured and compared to relevant experimental and theoretical results. The combined results established that the SLS mechanism with monodisperse, low-melting catalysts affords well-crystallized, narrowly dispersed nanowires of both III−V and II−VI semiconductors.

We have improved the SLS nanowire syntheses above and extended them to additional semiconductor materials including InAs, CdTe, and ZnTe, as described in a following section. In most of these cases, the nanowire diameters are controlled by the size of the catalyst nanoparticle, as has been described above for SFLS, VLS, and SLS growth. Interestingly, plots of nanowire diameter vs initial catalyst nanoparticle diameter are reasonably linear, as shown in Figure 5. Deviations from the lines can often be rationalized. Thus, the deviation of the small-diameter point for InP nanowires grown from In-catalyst nanoparticles (Figure 5, blue squares and blue dotted line) is a reflection of the instability and agglomeration tendency of small In nanoparticles under the reaction conditions.[10] This problem currently precludes growth of smaller-diameter wires from In catalysts. The spread in the large-diameter points for InP nanowires grown from 23-nm Bi-catalyst nanoparticles (Figure 5, red diamonds and red solid line) reflects significant variations in HDA/TOPO/TOP surfactant ratios during the initial optimization of the experimental conditions. The results indicate that factors other than the catalyst-nanoparticle size alone influence the nanowire diameter.

We suspect that additional mechanistic information is contained in the slopes and intercepts of the Figure 5 plots (Table 1). The (dotted) lines corresponding to nanowire growth from In-catalyst nanoparticles have intercepts near the origin and slopes of ca. 0.5, indicating that the nanowire diameters are approximately half the diameters of the catalyst nanoparticles from which they grew. In contrast, the (solid) lines corresponding to nanowire growth from Bi-catalyst nanoparticles have intercepts near 2 nm (except for ZnTe). The nonzero intercepts are consistent with a higher solubility of group V and VI elements in the Bi nanoparticles than in the In nanoparticles. Consequently, the Bi nanoparticles may dissolve additional semiconductor, swelling by a few nanometers in the initial alloying stage, before wire growth ensues. Interestingly, the lines for III−V nanowire growth from Bi nanoparticles lie close together with similar slopes of ca. 0.35, whereas the lines for II−VI nanowire growth from Bi nanoparticles lie close together with similar slopes of ca. 0.55. The mechanistic significance of the slopes is not clear, but they may be related to the contact angles that develop between the catalyst droplets and the semiconductor nanowires. All of the data in Figure 5 taken together indicate that nanowire diameters range from ca. 0.5−1.0 times the initial sizes of the catalyst nanoparticles, but they are never *larger* than the initial sizes of the catalyst nanoparticles, as is generally the case for VLS growth (see above).

Table 1. Slope and Intercept Values from Linear Fits of Nanowire Diameter vs Initial Catalyst Nanoparticle Diameter for SLS-Grown Wires (See Figure 5)

nanowire	catalyst	Figure 5 line	slope	intercept (nm)
InP	In	blue, dotted	0.46 ± 0.09	0.17 ± 1.05
GaAs	In	purple, dotted	0.58 ± 0.20	−0.29 ± 2.75
InP	Bi	red, solid	0.37 ± 0.02	2.16 ± 0.23
GaAs	Bi	black, solid	0.34 ± 0.04	2.59 ± 0.39
InAs	Bi	light green, solid	0.37 ± 0.01	2.60 ± 0.21
CdTe	Bi	gold, solid	0.52 ± 0.06	2.09 ± 0.63
ZnTe	Bi	dark green, solid	0.57 ± 0.04	1.15 ± 0.44

As our work has progressed, others have published studies on the SLS growth of 1D nanostructures. Mićić and co-workers[40] have described the growth of InP quantum rods from In-catalyst nanoparticles. Similarly, Ahrenkiel and co-workers[24] reported the preparation of InP quantum rods from an In self-catalyzed SLS process. Banin and co-workers[25,26] have grown InAs quantum rods by the SLS mechanism using Au-catalyst nanoparticles. Xie and co-workers[41−43] have reported SLS growth of GaP, InSb, and $CuInS_2$ nanorods. Korgel and co-workers[27,28] have grown Ge, GaP, InP, InAs, and GaAs nanowires from Bi-nanoparticle-catalyzed SLS growth but have not obtained narrow nanowire diameter distributions. Finally, Kuno and co-workers[33,34] have grown CdSe and PbSe nanowires by the SLS mechanism using Bi-catalyst nanoparticles, obtaining fascinating branched-wire structures.

Comparison of the Attributes of VLS, SLFS, and SLS Growth Methods. At the present stage of development, only tentative predictions can be made about relative strengths and weaknesses of the catalyzed nanowire growth methods. The results reported to date indicate that VLS, SFLS, and SLS growth methods are probably equally capable of producing narrow diameter distributions. Because VLS

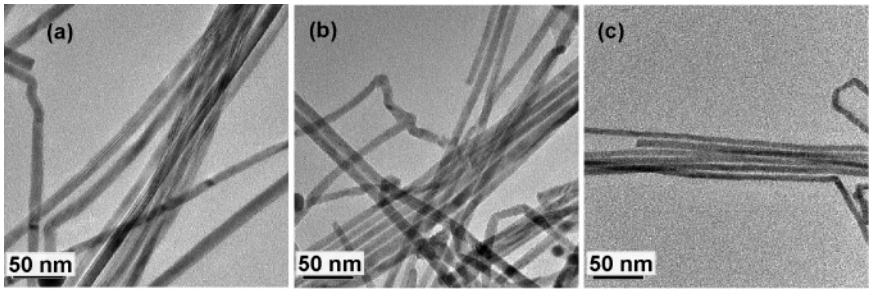

Figure 6. TEM images of SLS-grown InP nanowires with surface ligation consisting of MA, HDA, TOPO, TOP, and OPA. The quantity following the ± symbol is 1 standard deviation in the diameter distribution, expressed as a percentage of the mean diameter. Mean diameter = (a) 11.2 nm ± 17.5%, (b) 8.7 nm ± 21.8%, and (c) 5.9 nm ± 14.4%.

growth temperatures are the highest among the methods, VLS growth apparently affords the lowest crystalline-defect populations in the nanowires. VLS-grown III−V wires are longer and straighter than SLS-grown III−V wires. On the other hand, the solution-based SLS and SFLS methods allow surfactants (surface ligands) to be incorporated during growth. VLS-derived wires are grown without surfactants and likely acquire different surface reconstructions than are produced by the other methods. VLS-grown wires often have adventitious oxide coatings.[35] Because surface structure, ligation, and passivation influence the solubilities, luminescence characteristics, and likely also the electrical-transport behavior of nanowires, these properties may be best controlled by the SLS and SFLS methods. VLS growth generally affords mean diameters greater than 10 nm (although there are exceptions),[38] whereas SLS growth routinely affords mean diameters in the range of 4−10 nm. The origin of this difference appears to be the growth temperature. Semiconductors have higher solubilities in catalyst droplets at the higher VLS growth temperatures; thus, VLS catalyst droplets become more enlarged during the initial alloying stage[44] (see above) than do SLS catalyst droplets. Thus, SLS growth may have an advantage in providing smaller-diameter wires that exhibit stronger quantum-confinement effects. The VLS method likely has more synthetic generality. For example, SLS growth has not afforded high-quality oxide or nitride nanowires.[72] However, the SLS method is apparently the easiest to implement. SLS growth can be conducted in most inorganic or organometallic laboratories, whereas the SLFS and VLS methods require specialized apparatuses. Clearly, the SLS, SFLS, and VLS methods for nanowire growth are complementary and constitute useful alternatives to one another.

Synthetic Results for Specific SLS-Grown Semiconductor Nanowires

Indium Phosphide. The SLS InP-nanowire synthesis we previously reported[10] used a polymer surfactant to retain nanowire solubility. We sought a synthesis in which the InP nanowires would be stabilized by traditional quantum-dot surfactants to facilitate comparisons of nanowire spectroscopic properties to those of the corresponding InP quantum dots and rods. Thus, we recently developed the preparation given in eq 1.

$$\mathrm{In(myristate)_3 + P(SiMe_3)_3} \xrightarrow[\text{Bi nanoparticles}]{\text{240−300 °C polydecene}} \underset{\text{HDA, TOPO, TOP, OPA, DOA}}{} \text{InP nanowires} \quad (1)$$

Representative images of nanowires obtained from eq 1 are shown in Figure 6. The complex surfactant cocktail is necessary to produce wire specimens of good quality. We found empirically that HDA is very important for improving nanowire crystallinity and in promoting narrow diameter distributions. The surfactants TOPO and TOP produce straighter wires by reducing kink sites. The additive *n*-octylphosphonic acid (OPA) quenches the homogeneous nucleation of InP rod clusters, and di-*n*-octylamine (DOA) stabilizes small Bi-catalyst nanoparticles against aggregation. The In/P ratio in the precursors is also important; when the precursor In/P ratio is greater than ca. 1.5, In_2O_3 is produced. The optimal In/P ratio is 1.1−1.3.

The wires so obtained have controlled diameters in the range of 4−12 nm, with standard deviations in the diameter distributions of 13−21% of the mean diameters. The nanowire lengths are generally greater than 1 μm and depend on the reaction time; however, wires with the smaller diameters are significantly shorter. Reaction temperatures at the lower end of the indicated range (eq 1) are required to successfully grow thinner wires, and as the diameters decrease, the wires become kinkier. The nanowires are soluble and exhibit discernible excitonic features in their absorption spectra, comparable to those reported earlier.[10]

Indium Arsenide. SLS InAs-nanowire growth may be conducted similarly, as shown in eq 2 and Figure 7. The surfactants HDA and TOP greatly improve the diameter distributions, straightness, and crystallinity of the wires. TOP is especially useful for improving the quality of the smaller-diameter wires. Conversely, TOPO, even in small amounts, is deleterious to the quality of the InAs nanowires. They become short and excessively kinky.

$$\mathrm{In(myristate)_3 + As(SiMe_3)_3} \xrightarrow[\text{Bi nanoparticles}]{\text{260−300 °C, polydecene}} \underset{\text{HDA (TOP)}}{} \text{InAs nanowires} \quad (2)$$

The InAs nanowires are grown with controlled diameter in the range of 5−13 nm, with standard deviations in the

(72) Dingman, S. D.; Rath, N. P.; Markowitz, P. D.; Gibbons, P. C.; Buhro, W. E. *Angew. Chem., Int. Ed.* **2000**, *39*, 1470−1472.

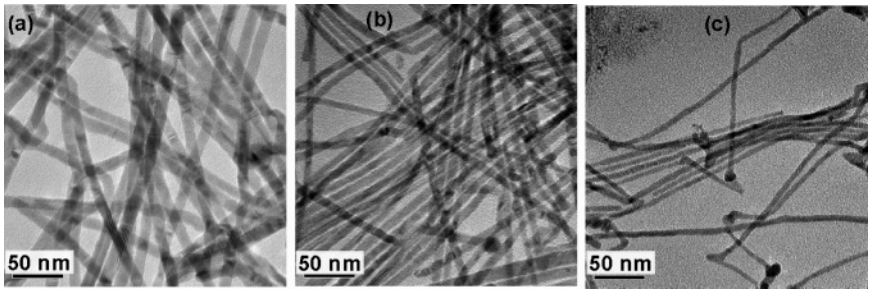

Figure 7. TEM images of SLS-grown InAs nanowires. The quantity following the ± symbol is 1 standard deviation in the diameter distribution, expressed as a percentage of the mean diameter. Mean diameter = (a) 11.5 nm ± 12.1%, (b) 8.8 nm ± 11.2%, and (c) 5.3 nm ± 12.4%.

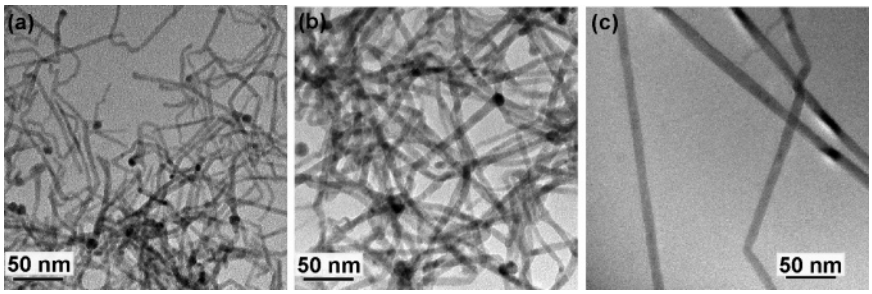

Figure 8. TEM images of SLS-grown GaAs nanowires. The quantity following the ± symbol is 1 standard deviation in the diameter distribution, expressed as a percentage of the mean diameter. Mean diameter = (a) 4.9 nm ± 15.5%, (b) 7.0 nm ± 12.7%, and (c) 9.2 nm ± 20.7%.

diameter distributions of 11−16% of the mean diameters. Their lengths are comparable to those of the InP nanowires described immediately above. As for the InP nanowires, growth temperatures at the low end of the indicated range (eq 2) are required for smaller-diameter wires. The spectroscopic properties of these nanowires have not yet been investigated.

Gallium Arsenide. SLS-derived GaAs nanowires are prepared according to eq 3. The solvent 1-octadecene (ODE) is important to the success of the synthesis because the corresponding procedure conducted in polydecene results in poorer-quality wires with low solubilities. The surfactant HDA is also deleterious to wire quality and is therefore avoided. The use of TOPO is necessary to achieve good diameter control, and TOP increases the wire quality.

$$\mathrm{Ga}(\textit{tert}\text{-butyl})_3 + \mathrm{As(SiMe_3)_3} \xrightarrow[\text{Bi nanoparticles}]{\text{255 °C, TOP/TOPO, ODE}} \text{GaAs nanowires} \quad (3)$$

Representative TEM images are shown in Figure 8. The SLS-grown III−V nanowires, especially with small diameters, contain more kinks and diameter fluctuations than do the SLS-grown II−VI nanowires described below. Clearly, the GaAs wires suffer from these problems to a greater extent than do the corresponding InP and InAs wires. Even so, they exhibit well-resolved excitonic features in their absorption spectra.

The diameters of the wires obtained from eq 3 are controlled in the range of 4.5−9.0 nm, with standard deviations in the diameter distributions of 16−20% of the mean diameters. The lengths are only 500−1000 nm, which are shorter than the other examples discussed here, but long enough for the wires to behave as 2D confinement systems (quantum wires).

By exchange of the traditional quantum-dot surfactants in eq 3 for a polymer surfactant and by omission of the Bi-catalyst nanoparticle, GaAs wires can be grown by a self-catalyzed SLS process, from Ga droplets. In this synthesis, the diameters are controlled by the reaction temperature and the amount of polymer employed. The wires so obtained are shorter (<300 nm) but straighter and exhibit more-prominent excitonic features in their absorption spectra.

Cadmium Selenide. We now use an adaptation of the procedure previously reported[6] for SLS growth of CdSe quantum wires (eq 4; TBP═Se = tri-*n*-butylphosphine selenide). The Cd precursor has been switched from cadmium stearate to cadmium oleate to improve nanowire solubility and is generated in situ from CdO and oleic acid. The surfactant HDA is employed to improve the photoluminescence quantum yields of the wires. The Cd/Se precursor ratio is an important synthetic parameter; we find that a ratio of 1:30 improves the wire length and straightness and enhances the photoluminescence as well.

$$\mathrm{Cd(oleate)_2} + \mathrm{TBP{=}Se} \xrightarrow[\substack{\text{HDA, TOP (TBP)}\\ \text{Bi nanoparticles}}]{\text{240−280 °C, TOPO}} \text{CdSe nanowires} \quad (4)$$

Representative TEM images of the SLS-grown CdSe nanowires are shown in Figure 9. The diameters are varied in the range of 4.7−15 nm, with standard deviations in the diameter distributions of 11−17%. In this case, the diameters are controlled by a combination of Bi-nanoparticle size and reaction temperature; that is, the nanowire diameters are quite sensitive to the growth temperature employed. The wires are generally several micrometers in length and can be as long as 10 μm. They are very straight and, apart from stacking faults, have near-single-crystal character.

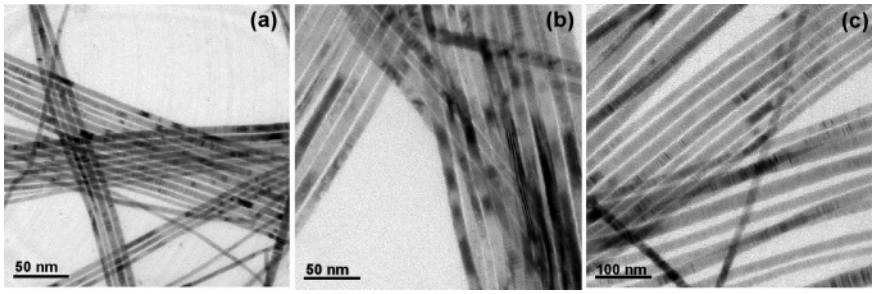

Figure 9. TEM images of SLS-grown CdSe nanowires. The quantity following the ± symbol is 1 standard deviation in the diameter distribution, expressed as a percentage of the mean diameter. Mean diameter = (a) 5.3 nm ± 14.4%, (b) 9.7 nm ± 11.8%, and (c) 17.2 nm ± 13.1%.

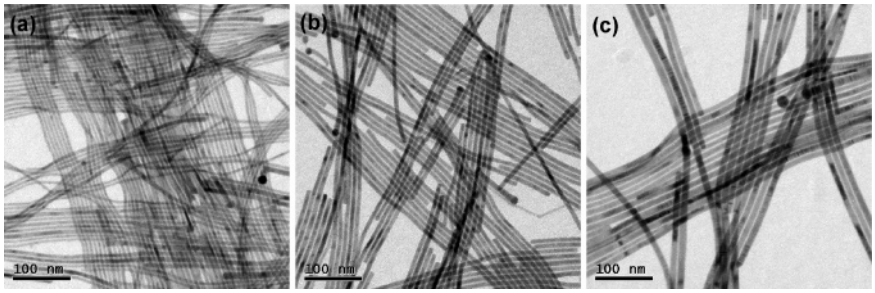

Figure 10. TEM images of SLS-grown CdTe nanowires. The quantity following the ± symbol is 1 standard deviation in the diameter distribution, expressed as a percentage of the mean diameter. Mean diameter = (a) 5.4 nm ± 22.2%, (b) 7.4 nm ± 12.2%, and (c) 9.7 nm ± 20.6%.

Cadmium Telluride. A cadmium alkylphosphonate precursor is preferred for the SLS growth of CdTe quantum wires, as shown in eq 5, which is generated in situ from CdO. This precursor is less reactive than are the corresponding cadmium carboxylates, and its use eliminates a side reaction that produces CdTe quantum dots. Cd/Te precursor ratios of ca. 5:1 produce the best wires. Technical-grade TOPO is not a suitable solvent; we use distilled TOPO. The reaction temperature is varied in the indicated range according to the size of the Bi nanoparticles employed, with lower temperatures for smaller Bi nanoparticles. The CdTe quantum wires exhibit well-resolved absorption spectra.

$$\mathrm{Cd(ODPA)} + \mathrm{TOP{=}Te} \xrightarrow[\text{Bi nanoparticles}]{240-320\ ^\circ\mathrm{C,\ TOPO}} \mathrm{CdTe\ nanowires} \quad (5)$$

TEM images of the CdTe wires are shown in Figure 10. The diameters are controlled in the range of 5−20 nm, with standard deviations in the diameter distributions of 10−22%. The average lengths are several micrometers, and wires as long as 20 μm have been observed. The images reveal a strong tendency of the wires to align in parallel bundles, presumably as a result of van der Waals attractions. The white space between adjacent wires evident in the images of such bundles is due to the TOPO-surfactant coatings on the wires. The wires are of excellent crystalline quality.

Zinc Telluride. The reactions for SLS growth of ZnTe wires are shown in eqs 6 and 7. The solvent ODE is much preferred over polydecene, which results in wires of low solubility and increased atmospheric sensitivity. The tellurium precursor TOP═Te may not be used in place of TBP═Te. The surfactant HDA results in wider diameter distributions. Equation 6 produces nanowires of diameter 5−12 nm, whereas eq 7 produces smaller-diameter wires in the range of d = 3.7−5.0 nm. Apparently, the more-reactive precursor $ZnEt_2$ assists in the growth of the small-diameter wires. The surfactant TOP improves the wire quality for eq 6 but not for eq 7 and should not be used.

$$\mathrm{Zn(stearate)_2} + \mathrm{TBP{=}Te} \xrightarrow[\text{Bi nanoparticles}]{290\ ^\circ\mathrm{C,\ TOPO/TOP,\ ODE}} \mathrm{ZnTe\ nanowires} \quad (6)$$

$$\mathrm{ZnEt_2} + \mathrm{TBP{=}Te} \xrightarrow[\text{Bi nanoparticles } (d = 4.8\ \text{nm})]{270-280\ ^\circ\mathrm{C,\ TOPO,\ ODE}} \mathrm{ZnTe\ nanowires}\ (d < 5\ \text{nm}) \quad (7)$$

Images of the ZnTe wires are shown in Figure 11. The standard deviations in the diameter distribution range from 14 to 20% of the mean diameters, which are 3.7−12 nm. The wire lengths are 1−3 μm. Absorption spectra of the wires exhibit well-resolved excitonic features, especially for the smaller-diameter specimens.

Future Challenges

We previously referred to SLS growth as a "nearly general" strategy for the synthesis of soluble, diameter-controlled semiconductor nanowires. This qualification is necessary because, as the previous section reveals, much trial-and-error empiricism is still required to extend the SLS method to each new family of nanowires. A set of general guidelines for universally applicable SLS reaction conditions, solvents, precursors, and surfactants has not yet emerged, and we hope to develop such guidelines in the future.

Several aspects of the SLS synthesis of semiconductor nanowires require further improvements. The quality of the III−V nanowires so far produced by SLS growth is not as good as that of VLS-grown III−V nanowires,[37] III−V

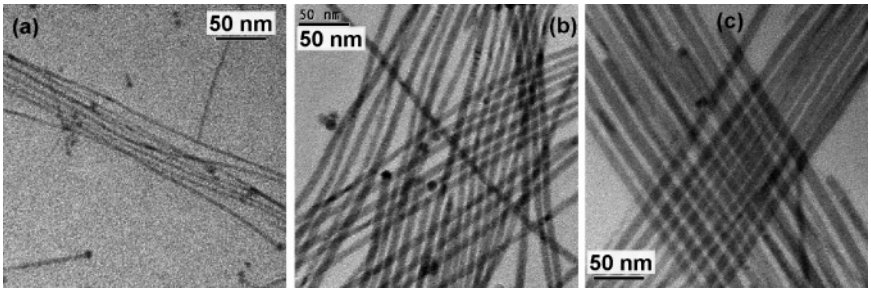

Figure 11. TEM images of SLS-grown ZnTe nanowires. The quantity following the ± symbol is 1 standard deviation in the diameter distribution, expressed as a percentage of the mean diameter. Mean diameter = (a) 3.7 nm ± 17.1%, (b) 7.6 nm ± 13.8%, and (c) 11.1 nm ± 15.8%.

quantum dots,[73] and SLS-grown II−VI quantum wires. Lower crystalline-defect populations in all of the SLS-derived quantum wires are desirable. Nanowire diameters in the range of ca. 1.5−5 nm would greatly benefit quantum-confinement studies, but controlled growth in this diameter range has proven difficult. Clearly, important synthetic challenges remain.

Surface passivation (ligation) is a major issue because optical properties such as photoluminescence are strongly dependent on it. However, the nanowire surface structure and the quantities and precise identities of surface ligands are poorly understood. In the SLS synthesis, nanowires are grown in a broth of excess surfactant. When they are precipitated and washed after growth, photoluminescence efficiencies decrease, often by a lot. Thus, the purification and even the definition of the purity for nanowires are issues that must be addressed. To date, the maximum ensemble quantum yields we have measured for SLS-grown quantum wires are only ca. 2%. However, we have estimated single-wire quantum yields for bright nanowires of ca. 20%. Single-nanowire microscopy and spectroscopy reveal that the luminescence behavior within nanowire specimens is quite heterogeneous. We believe that this heterogeneity is a reflection of uneven, nonideal surface passivation, which we are working hard to improve.

Finally, as noted above, the emergence of the nanowire field has stimulated much interesting science and excitement for potential applications. However, nanowire devices are currently fabricated in a one-at-time serial manner.[18,19,23] The development of methods for the massively parallel integration of nanowire structures will be necessary for the field to have a real-world impact. Until then, nanowire technology will remain a somewhat distant dream.

Acknowledgment. We are grateful to the National Science Foundation for funding this work for the past several years, currently under Grant CHE-0518427. We thank our collaborators Prof. Richard A. Loomis, Dr. Jingbo Li, Dr. Lin-Wang Wang, Prof. Patrick C. Gibbons, Dr. Nigam P. Rath, Prof. K. F. Kelton, and Prof. R. M. Penner, who participated in these studies. We also fondly acknowledge the contributions of our former co-workers Dr. Subhash C. Goel, Dr. Kathleen M. Hickman, Dr. Timothy J. Trentler, Dr. Ann M. Viano, Dr. Paul D. Markowitz, Dr. Michael P. Zach, and Dr. Sean D. Dingman.

IC060498R

(73) Mićić, O. I.; Jones, K. M.; Cahill, A.; Nozik, A. J. *J. Phys. Chem. B* **1998**, *102*, 9791−9796.